Band 22, Heft 2 (1986), S. 101—124

ZEITSCHRIFT FÜR GLETSCHERKUNDE UND GLAZIALGEOLOGIE

ABHANDLUNGEN

SENSITIVITY STUDIES WITH A MASS BALANCE MODEL INCLUDING TEMPERATURE PROFILE CALCULATIONS INSIDE THE GLACIER

By W. GREUELL and J. OERLEMANS, Utrecht

With 9 figures

ABSTRACT

The aim of the present investigation is to gain more insight into the ablation process on alpine glaciers. This was done by means of experiments with a universally applicable computer model of the surface energy budget. In this model the turbulent energy fluxes at the surface are parameterized according to the Monin-Obukhov similarity theory and temperature and density profiles in the upper 25 m of snow/ice are calculated. Percolation and refreezing of meltwater is dealt with in a schematic way. The daily cycle is calculated explicitly. For the experiments presented here climatological data from Sonnblick (Austria, 3106 m) were used as input to the model.

The daily cycle of a typical summer day is discussed. We conducted several experiments to show the basic sensitivity of ablation to variations in atmospheric temperature, humidity, cloudiness and wind velocity. It appears that none of these variations can be neglected. The mass balance for a measurement year is presented for elevations ranging from 2000 till 3600 meters and for two different formulations of the turbulent fluxes. At lower elevations the choice of the formulation appears to have dramatic effects. In another experiment a comparison was made between the present model and models which calculate ablation with the assumption that the temperature of the glacier surface always remains at the melting point. It turns out that this "zero degree assumption" produces substantial errors when the ablation season is short. We finally discuss the effect of a heavy snowfall event in summer (of 5 cm water equivalent). It reduces ablation by about 8 cm water equivalent due to increased albedo. So the initial mass balance perturbation is nearly trebled.

EMPFINDLICHKEITSSTUDIEN MIT EINEM MASSENBILANZMODELL EINSCHLIESSLICH BERECHNUNGEN DES TEMPERATURPROFILS INNERHALB DES GLETSCHERS

ZUSAMMENFASSUNG

Das Ziel der vorliegenden Arbeit ist eine tiefere Einsicht in den Ablationsprozeß auf alpinen Gletschern zu bekommen. Für diesen Zweck wurde ein relativ kompliziertes, universell brauchbares Computermodell der Energiebilanz der Gletscheroberfläche entworfen. Die turbulenten Energieflüsse an der Oberfläche werden mit Hilfe der Monin-Obukhov-Theorie formuliert, Profile der Temperatur und Dichte werden für die obersten 25 m Schnee/Eis berechnet, das Durchsickern und Wiedergefrieren des Schmelzwassers wird schematisch berücksichtigt. Für alle Komponenten werden Tagesgänge berechnet. Für die vorliegenden Experimente wurden klimatologische Daten vom Sonnblick (Österreich, 3106 m) in das Modell eingegeben.

Der Tagesgang eines typischen Sommertags wird diskutiert. Wir haben mehrere Experimente ausgeführt, um die Empfindlichkeit der Ablation für Änderungen der Lufttemperatur, Feuchtigkeit, Bewölkung und Windgeschwindigkeit zu überprüfen, nach denen keine dieser Variablen demnach vernachlässigt werden kann. Die Massenbilanz eines Jahres wird für Höhen von 2000 bis 3600 m gezeigt, und zwar für zwei Formulierungen der turbulenten Flüsse. In den tieferen Lagen hat die Wahl der Formulierung einen beträchtlichen Einfluß auf die berechnete Ablation. In einem weiteren Experiment wird ein Vergleich zwischen dem vorliegenden Modell und Modellen gemacht, in welchen zur Ablationsberechnung vorausgesetzt wird, daß die Temperatur der Gletscheroberfläche immer auf dem Gefrierpunkt bleibt. Es stellt sich heraus, daß die letztere Bedingung wesentliche Fehler mit sich bringt, wenn die Ablationsperiode kurz ist. Zum Schluß diskutieren wir die Folgen eines Sommerschneefalls (5 cm Wasseräquivalent). Wegen der erhöhten Albedo wird die Ablation um ungefähr 8 cm Wasseräquivalent reduziert und die Störung der Massenbilanz somit fast verdreifacht.

1. INTRODUCTION

The ablation process on glaciers or other snow covered areas can be studied for a number of reasons. One is the prediction of run-off from catchment areas which may be especially useful in planning hydro-electric power production. Another reason for studying ablation on glaciers is the role that the mass budget plays in the relation between climate and glaciers length and volume. The present investigation is meant to deepen our understanding of this relation.

For this purpose a computer model simulating ablation is needed which should be used to study the sensitivity of ablation and ablation related processes to both relevant input parameters (geographical and meteorological) and to different model formulations. In order to facilitate the investigation of a large number of effects, the model should include a great number of relevant physical processes. Another requirement set to the model was universal applicability.

A number of models to calculate ablation have been proposed in the literature. Among them are index models, such as degree day models (see e. g. Harstveit 1984 and Braun 1985), and models which use an energy-balance approach (e. g. Ambach 1965, de la Casinière 1974 Escher-Vetter 1980, Hogg et al. 1982, Harstveit 1984 and Braun 1985). Index models did not seem to be suitable for the present investigation. They are black box models in which many physical processes are put together without universal applicability as they are, more than energy approach models, based on tuning to local conditions. Even most of the existing energy-balance models were thought to be too restrictive for the present investigation. The model we constructed is an extension of existing energy-balance models, incorporating of course many ideas of the existing models. Our model emphasizes the following points:

- The Monin-Obukhov similarity theory in which the boundary layer stratification affects the transfer coefficients, is applied in the computation of the turbulent fluxes. In most other models sensible and latent heat flux are proportional to the gradients of potential temperature and mixing ratio, respectively, regardless of stratification.
- In the present model the radiative fluxes are parameterized by equations which are as independent of locality as possible. The equations include factors like cloudiness, aspect, snow density (albedo), air temperature and humidity, etc.
- Most models keep the temperature of the glacier surface at the melting point. In reality the upper layers of the snow/ice even on a temperate glacier will cool during the accumulation season and in many nights of the ablation season (see

Wagner 1980). This means that ablation in 'zero degree models' starts too early in the morning during the ablation season and also that the ablation season as a whole starts too early, namely as soon as the total surface energy flux becomes positive. Apart from this, the temperature of the surface affects the outgoing radiative flux and the turbulent fluxes. In the present model the temperature profile inside the glaciers is calculated down to a depth of about 25 m, where the seasonal variation becomes negligible. As conductivity is correlated to density, density is carried as a dependent variable in the model. The density computation also offers the opportunity to parameterize albedo, since a correlation between density and albedo exists. Apart from being a more realistic approach, modelling of the temperature profile is an interesting topic on its own.

The following experiments will be presented here. The input parameters used are intended to represent conditions in the Alps. First, the daily cycle on a typical summer day near the equilibrium line will be presented. Then, the basic sensitivity to some meteorological input parameters will be shown. Thereafter, the yearly cycle at different elevations will be investigated for two different parameterizations of the turbulent fluxes so that the effect of the use of the Monin Obukhov similarity theory can be estimated. Further, the influence of the temperature calculations inside the glacier on the computed ablation will be investigated. The last experiment is concerned with the ablation-reducing effect of a heavy snow fall event in summer.

2. FORMULATION OF THE SURFACE HEAT FLUXES

A. INTRODUCTION

The model essentially consists of 2 parts. The first part computes the energy fluxes between atmosphere and glacier; the second part computes the energy fluxes inside the glacier, combined with mass transfer processes and phase changes inside and at the surface of the glacier. Strictly spoken, it is not a point model, but a one-dimensional model, because energy and mass transfer in the direction normal to the surface are computed in the uppermost layers (some 25 meters) of the glacier. This is described in section 3. In the absence of accumulation and rain the energy flux between atmosphere and glacier, Q_{ag}, consists of 4 individual contributions:

$$Q_{ag} = R_s + R_l + H + S \tag{1}$$

with R_s: short wave radiation flux
R_l: long wave radiation flux
H: turbulent transfer of sensible heat
S: turbulent transfer of latent heat

Fluxes from the atmosphere towards the glacier are regarded as positive.

B. SHORT-WAVE RADIATION

The global radiation on a horizontal surface which is not screened by the horizon is determined by the sun-earth distance, by the solar zenith angle and by the respective distributions of temperature, water vapour, ozon, clouds and aerosols in the atmosphere. Cloud type and aerosol size distribution also affect the global radiation. The parameterization of the global radiation ($R_s\downarrow$) for clear skies is taken from Meijers and Dale (1983). In this formulation no distinction is made between direct and diffuse short wave incoming radiation. It is only valid when the sun is above the horizon, of course:

$$R_s\,(n=0)\downarrow = I_0 T_R T_g T_w T_{as} \cos(z_s) \tag{2}$$

with n: cloudiness
- I_0: extraterrestrial flux density at the top of the atmosphere on a surface normal to the incident radiation.
- z_s: angle between the incident ray and the normal to the surface. Formulae for z_s are given by Escher-Vetter (1980).
- T_i: transmission coefficients for Rayleigh scattering (R), absorption by gases other than water vapour (g) and water vapour (w), and absorption and scattering by aerosols (as).

The values of I_0 and z_s at any place and time can accurately be computed from astronomical formulae. Since the distribution of gases, except for water vapour is fairly constant the product $T_R T_g$ is merely a function of the solar zenith angle and the atmospheric pressure at the location for which the computations are made. T_w is determined by the distribution of water vapour in the atmosphere and by the solar zenith angle:

$$T_w = 1 - 0.077\,(u\,m)^{0.3} \tag{3}$$

with u: total water vapour in a vertical column of the atmosphere in cm
- m: optical air mass

The total water vapour is estimated from the mixing ratio at screen height, w_a (Smith 1966):

$$u = \frac{p_0 w_a}{g\lambda} \tag{4}$$

with p_0: atmospheric pressure in Pa
- g: gravity in m s^{-2}
- λ: a constant, determined by the vapour distribution ($\lambda = 3.79$ in this study)

The amount of aerosol in the atmosphere at locations situated at an altitude far above sea level, is usually small. As long as only 'high' glaciers are considered like in this study, the attenuation by aerosols can be neglected.

The attenuation of the global radiation by clouds is represented by the transmission coefficient T_c:

$$R_s(n)\downarrow = T_c R_s(n=0)\downarrow \tag{5}$$

In this study T_c is empirically related to cloudiness, elevation of the location and time of the year. Formulae were computed by approximating data given by Sauberer (1955) by polynomials of order 3. Fig. 1 gives T_c as a function of cloudiness for different times of the year at 3000 m a.s.l. Apparently the effect of clouds on the global radiation varies through the year. For equal cloudiness the average attenuation is largest in August and September ($T_c = 0.35$ for overcast skies) and smallest in April and May

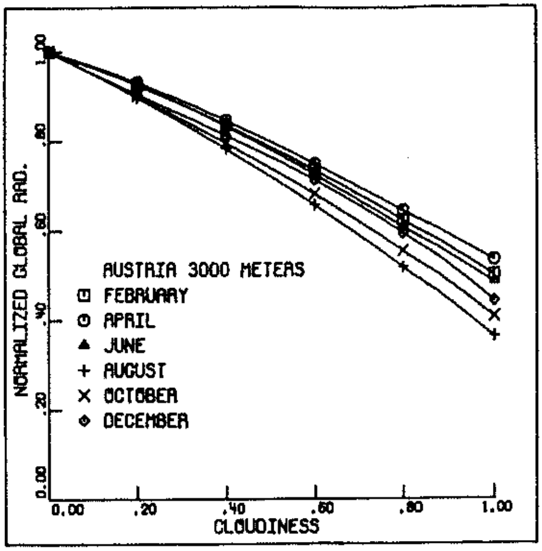

Fig. 1: Variation of T_c with cloudiness at 3000 m a.s.l. for different months of the year according to data from Sauberer (1955)

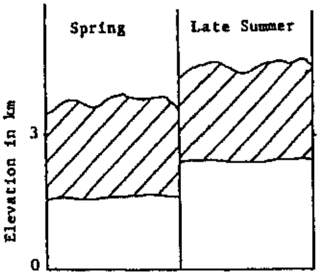

Fig. 2: Schematic figure showing the different averaged cloud distribution during spring and late summer. Hatched areas are clouds

($T_c = 0.54$ for overcast skies). This may be explained by systematic differences in cloud type. In general, clouds have a lower base and top in spring than in late summer. The situation is illustrated in fig. 2. Both situations depicted here, will be described by an observer as overcast, at sea level as well as at 3000 m altitude. At 3000 m however, the attenuation will be less in the spring situation than in the late summer situation, because the path of the sun rays through the clouds is shorter. With this argument in mind, one expects the seasonal variation to decrease with decreasing altitude. This indeed appears to be the case. The influence of elevation on the yearly-averaged value of T_c is shown in fig. 3.

In the present model, T_c is computed by means of the following scheme:

- for given cloudiness the yearly averaged T_c was computed for 2000 and 3000 m altitude according to the polynomials calculated from Sauberer's data.
- the yearly averaged T_c at the altitude of the site is linearly interpolated or extrapolated from the transmission coefficients at 2000 and 3000 m.
- the seasonal variation was calculated by taking into account a correction, which varies sinusoidally with the time of the year with an amplitude, which is independent of altitude and varies linearly with cloudiness:

$$\Delta T_c = c_1 \, n \sin(\omega t) \tag{6}$$

with ΔT_c: correction term for seasonal variation

c_1: amplitude of variation for overcast skies

t: time

ω: annual frequency

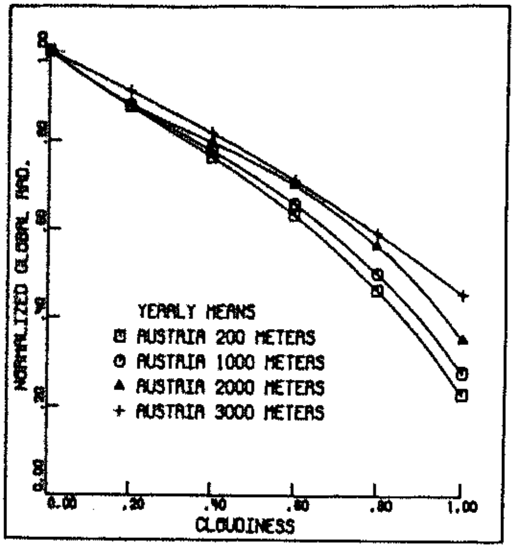

Fig. 3: Yearly mean values of T_c as a function of cloudiness for four different elevations according to data from Sauberer (1955)

The outgoing short wave radiation ($R_s\uparrow$) is the product of the global radiation ($R_s\downarrow$) and the albedo (α). The albedo is dependent on the state of the glacier surface and on the ratio of the direct and the diffuse part of the global radiation. Albedo is generally lower for higher density and wetness of the surface and for lower cloudiness and incident angle. The parameterization of the albedo used in this study reads:

$$\alpha = 0.79 - 0.5 \cdot 10^{-3} \rho_o + 0.07 \exp(-M/0.5) + 0.07\, n + 0.07\,(1.225 - 1.3 \cos(z_s))\,(1 - n) \tag{7}$$

where ρ_o: density of snow/firn/ice at the surface in kg m^{-3} (both albedo and density are to a great extent determined by the state of metamorphosis)

M: the amount of meltwater in mm water equivalent produced during one time step (30 minutes)

z_s: angle between the direct sun ray and the normal to the surface

n: cloudiness

This relation was detained from the data and considerations mentioned in Dirmhirn and Trojer (1955) and Dirmhirn and Eaton (1975). It should be noted that the values of the coefficients in this relation are based on data that were not systematically acquired to test such a relation. We expect, however, that it will be accurate enough for the present study.

C. LONG WAVE RADIATION

The long wave radiation was modelled according to Kimball et al. (1982). Since the glacier surface radiates almost as a black body, we have:

$$R_l\uparrow = \sigma T_o^4 \tag{8}$$

with $R_l\uparrow$: outgoing long wave radiation
σ: Stefan Boltzmann's constant
T_o: temperature of the glacier surface in K

The incoming long wave radiation for clear-sky conditions (R_a) is computed from:

$$R_a = \varepsilon_a \sigma T_a^4 \tag{9}$$

with ε_a: full-spectrum, clear sky emittance
T_a: temperature of the atmosphere at screen height in K.

The expression for ε_a reads:

$$\varepsilon_a = 0.70 + 5.95 \cdot 10^{-7}\, e_a \exp(1500/T_a), \tag{10}$$

where e_a is the screen level vapour pressure in Pa. These empirical formulae were inferred from data taken at lower altitudes. However, they should be applicable also at higher altitudes, since almost all of the incoming long wave radiation is received from the atmospheric layer just above the surface (Geiger 1966).

The contribution from the clouds (R_c) is considered as a correction to the clear-sky radiation.

$$R_l\downarrow = R_a + R_c, \tag{11}$$

where $R_l\downarrow$ denotes the long-wave incoming radiation. In this study it is assumed that all clouds are in one layer. Then R_c may be parameterized as follows:

$$R_c = \sigma T_{cl}^4\, \varepsilon_c\, n\, f_8\, \tau_8, \tag{12}$$

with σT_{cl}^4: black body radiation from the cloud layer, where T_{cl} is the temperature of the base of the cloud layer in K
ε_c: cloud emittance. A value of 0.8 was taken. For dense cloud types ε_c is close to 1.0; for cirrus ε_c is on average close to 0.5
n: cloudiness
f_8: fraction of black body radiation emitted in the atmospheric window (8—14 μm) that can be transmitted to the surface
τ_8: transmittance of the atmosphere in the 8—14 μm window. It can be estimated from temperature and vapour pressure at screen height.

Thus, R_c is a function of T_{cl}, T_a, n and e_a. The variables T, n and e_a belong to the standard input of the model, whereas T_{cl} is inferred from T_a, an assumed altitude of the cloud layer (4000 meters) and a lapse rate (−0.65 K/100 m). These values should represent average conditions.

D. TURBULENT FLUXES

These fluxes were computed by means of the Monin-Obukhov similarity theory (M. O.-theory, hereafter). Measurements show that for a given height above the surface and a given wind velocity, sensible and latent heat flux are not simply proportional to the gradients of potential temperature and vapour pressure respectively, as assumed in many studies. The M. O.-theory takes into account the influence of stratification on the transfer coefficients K_H and K_S, which relate the turbulent fluxes linearly to the gradients. Relative to the models that use transfer coefficients which are independent of stratification (s. i.-theory, hereafter), it predicts a larger exchange for unstable stratifications and a smaller exchange for stable stratifications (see fig. 4). The fluxes even vanish for very stable conditions (low wind speeds, large temperature gradients). A description of this similarity theory is given by for instance Businger (1973) and by Kraus (1972), who discusses the application to glaciers. Itier (1980) presents the iteration scheme used in the present study for the actual computation of the fluxes. Values of the surface roughness parameters for wind ($z_0 = 1.33 \cdot 10^{-3}$ m) and for temperature and water vapour pressure ($r_0 = s_0 = 10^{-5}$ m) were taken from Hogg (1982).

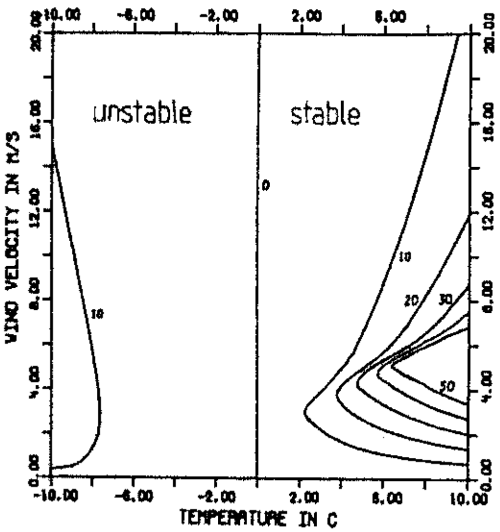

Fig. 4: Contour plot of the difference in sensible heat flux predicted by the s. i.-theory and by the M. O.-theory. Figures along contours give absolute values in W/m². On the abscissa is the temperature difference between a height of 2 m above the surface and the surface, on the ordinate the wind velocity at a height of 10 m

3. PROCESSES INSIDE AND AT THE SURFACE OF THE GLACIER

A. THE ENERGY BUDGET

The rate of temperature change inside the glacier is described by the following energy conservation law:

$$\rho\, c_p \left(\frac{\partial T}{\partial t} + w \frac{\partial T}{\partial z}\right) = \frac{\partial}{\partial z}\left(K \frac{\partial T}{\partial z}\right) + W \qquad (13)$$

with ρ: density
c_p: specific heat capacity at constant pressure
T: temperature
w: velocity normal to the surface
z: coordinate of direction normal to the surface
K: conductivity
W: energy release by phase changes

Thus, the local rate of temperature change is determined by conduction and advection of snow/ice normal to the surface and by the energy release or consumption by phase changes. The equation holds in the upper layers, which are considered in this study (some 25 m), because here advection and conduction parallel to the surface and energy release by deformation can be neglected for the present purpose. Boundary conditions are given by the energy flux from atmosphere to glacier (equation 1) and by a zero heat flux at the lower boundary of the model. Penetration of radiation is neglected in this study. K can be estimated from the density (ρ in kg/m^3), see Paterson (1981):

$$K = 2 \cdot 1.10^{-2} + 4.2 \cdot 10^{-4} \rho + 2.2 \cdot 10^{-9} \rho^3 \; (\mathrm{W\,m^{-1}\,K^{-1}}) \tag{14}$$

B. MASS TRANSFER AND PHASE CHANGES

Phase changes play a very important role in the energy budget. If the temperature of the snow is at the melting point, any available energy will be used for melting. If penetration of radiation and energy supplied by deformation are neglected as in this study, this only occurs at the surface. In this study all meltwater is allowed to penetrate downwards, until it reaches a layer with a density exceeding 800 kg m^{-3}. In that case it runs off. On its way downwards the meltwater may refreeze in layers with a temperature below 0°C. The effects of this process are considered by the following scheme: if the meltwater reaches a model layer with a temperature below 0°C, this layer is warmed up by refreezing the meltwater. If the resulting temperature exceeds 0°C, the temperature is put equal to 0°C and the remaining amount of meltwater is computed. This meltwater penetrates downwards into the next model layer, etc. After penetration through the lowermost layer the remaining meltwater runs off. So, if the temperature is equal to 0°C in all layers, all meltwater is allowed to run off. The effect of the refreezing process on snow density is also taken into account. The velocity of percolation is not considered. This seems to be a reasonable approach, because the penetration velocity of water in snow (Ambach et al. 1981) is much greater than the velocity of a temperature wave.

The contribution of phase changes to the energy flux at the glacier surface has already been taken into account by the latent heat flux in equation 1. The specific latent heats of vapourization and sublimation are used for melting and frozen surfaces, respectively. The effect of freezing rain is neglected. This can be done as long as the whole glacier ist at 0°C during a rain event. For temperate glaciers this will often be the case. Thus, the run off is the sum of the liquid precipitation and the meltwater formed at the surface, minus the refrozen meltwater. Ablation is the sum of run off and sublimation, minus condensation and rain.

C. THE DENSITY PROFILE

Densification by metamorphosis is formulated as follows:

$$\Delta\rho_i = (910 - \rho_i)(c_2 + c_3 M(\Delta t))\Delta t \tag{15}$$

where $\Delta\rho_i$ = density increase in kg m^{-3} during time Δt for model layer i
M = amount of meltwater during Δt in mm water equivalent
c_2 = $9 \cdot 10^{-3}$ day^{-1} and $c_3 = 3 \cdot 10^{-3}$ day^{-1} mm^{-1} for $\rho < 300$ kg m^{-3}
c_2 = $4.5 \cdot 10^{-4}$ day^{-1} and $c_3 = 1.5 \cdot 10^{-4}$ day^{-1} mm^{-1} for $\rho \geqslant 300$ kg m^{-3}

So the rate of densification decreases with increasing density and is proportional to a parameter c_2, representing the metamorphosis in the absence of meltwater. In the presence of meltwater the rate of change is much larger. Some 20 mm a day, which is the order of magnitude of the amount of meltwater during a summer day close to the equilibrium line in the Alps, will increase the rate of change by about a factor 7. Equation 15 is applied to all model layers. Although the rate of density change is expected to be depth- (i. e. pressure-) dependent, this effect is disregarded in the present study. In order to allow a rapid initial density increase, different values of the constants are used for densities greater than and less than 300 kg m^3.

Other processes affecting the density profile were also taken into account, namely ablation, refreezing meltwater (see subsection 3 b) and snow fall. The density of fresh snow is assumed to be 100 kg m^{-3}.

This treatment of density changes is admittedly crude, but one should bear in mind that the density calculations themselves are no aim of the present study.

4. SOME MODEL SPECIFICATIONS

The evolution of the temperature profile is calculated by solving equation 13 numerically with an implicit scheme. The time step is the same as used for the calculation of the surface energy fluxes, namely 30 minutes.

In order to save computer time, the density profile is adjusted only once a day, at midnight. This is done as follows:

- calculation of density and thickness change of each model layer as caused by metamorphosis by means of equation 15. Thus, Δt is equal to 24 hours in equation 15.
- calculation of the effect of melting and snow fall during the past 24 hours. Layers disappear and/or are reduced by melting and a new layer is added on top of the existing model layers in the case of snow fall.
- discretization of temperatures and densities at the new grid points. Every day the grid points must be specified again, because the position of the grid is relative to the surface and thus is moving relative to material points. The grid consists of 42 points. The grid point distance increases from 6 cm at the top of the model to about 5 m at the bottom.

The effect of refreezing meltwater on temperatures and densities is computed every 30 minutes.

5. EXPERIMENTS

A. INTRODUCTION

For the experiments input data representative for alpine glaciers were needed. We used observations from the meteorological station Sonnblick in Austria (elevation 3106 m, latitude 47°03′ N, longitude 12°57′ E), see table 1. Except for precipitation, the variability of daily weather was not taken into account. This implies that all statements and conclusions made from now on are only valid for 'climatological weather', unless explicitly mentioned otherwise. When running the model for other elevations, temperatures were adjusted by assuming a constant lapse rate of − 0.0065 K/m. All other input parameters remained unchanged except for humidity which was calculated by assuming a constant relative humidity with height. Special attention was given to the simulation of precipitation. Cehak and Withalm (1980) investigated the application of a Markov chain model to the simulation of the occurrence of precipitation on Sonnblick. They found that the probability of a day being dry or wet is only dependent on the length and the state of the dry or wet period before that day. The simulation in the present model is based on this conclusion. Transition probabilities after a certain number of wet or dry days were calculated from table 1 of Cehak and Withalm (1980).

Tab. 1: Climatic table for Sonnblick

month	temperature in °C mean	daily range	mean vapour pressure in mbar	cloudiness	wind velocity in m/s	precipitation (in mm)
Jan.	−13.2	4.7	1.8	0.67	7.3	115
Feb.	−13.0	4.7	1.8	0.67	7.1	108
Mar.	−11.2	4.6	2.2	0.70	6.7	112
Apr.	− 8.2	4.6	3.0	0.77	5.8	153
May	− 3.8	4.3	4.3	0.81	5.2	136
June	− 0.6	4.3	5.5	0.80	5.1	142
July	1.6	4.4	6.4	0.78	5.1	154
Aug.	1.4	4.3	6.3	0.74	5.2	134
Sep.	− 0.5	4.0	5.2	0.67	5.5	104
Oct.	− 4.3	4.0	3.7	0.65	6.2	118
Nov.	− 8.3	4.0	2.8	0.66	6.6	108
Dec.	−11.4	4.4	2.1	0.65	6.8	111
Annual	− 6.0	4.4	3.8	0.71	6.0	1495

Further, it is assumed that the distribution of the amount of precipitation on wet days can be described by an exponential probability law. Precipitation is solid if the daily mean temperature is below zero, and liquid if the daily mean temperature is above the melting point.

B. DIAGNOSIS OF THE DAILY CYCLE

First, a diagnosis of the daily cycle was made at the altitude of the station. The results for a typical summer day (July 15) are presented here (see fig. 5). As input the climatological data for July were used (see table 1). Like in all other experiments cloud height was 4000 meters and the glacier surface was horizontal. Initial density

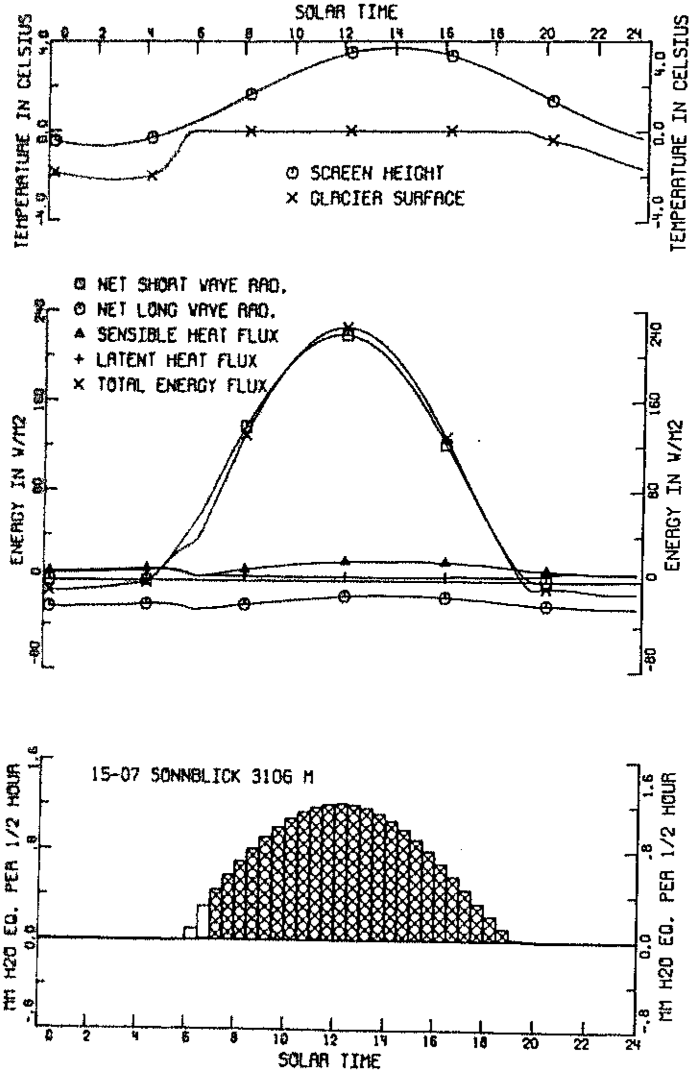

Fig. 5: Variation of temperatures, surface energy fluxes, formation of meltwater and ablation with time for 'climatological' data for July at Sonnblick (see text)

($500\ kg\ m^{-3}$) and temperature (0°C) were uniform throughout the model layers. The simulation started at noon, July 14.

The upper part of fig. 5 shows the temperatures of the atmosphere at screen height (input) and of the glacier surface (calculated). The stratification is stable all through the day. The tendency to instability during day time is suppressed by the fact that the temperature of snow/ice has a maximum of 0°C. Experiments with climatological means for other months show that unstable stratifications only occur from February till June, during day time, when the relatively strong short wave radiation raises the surface temperature above the low atmospheric temperature.

In the middle of fig. 5 the surface energy fluxes are shown. During summer days the total energy flux is dominated by the short wave radiation. The relative contributions of the daily-averaged fluxes are (net short wave radiation = 100 %): net long wave radiation = −25 %, sensible heat flux = 14 %, latent heat flux = 6 %. The average heat conduction upwards is very small (4 %). This flux is not necessarily zero when averaged over an entire day, because refreezing meltwater transports heat downwards.

The lower part of fig. 5 shows the amount of meltwater formed at the surface (total areas of the columns) and the amount of ablation (hatched areas) for periods of half an hour. The only major difference between these variables is between 5:30 and 7:00 a.m. (solar time). The sun rises at about 4:30. Thereafter the total surface energy flux soon becomes positive and, in the present model, it starts to heat up the snow. Shortly before 5:30 the temperature at the surface is raised to the melting point and the first meltwater is formed. This percolates and heats the snow underneath, untill at about 6:45 the snow is at the melting point in all layers. The ablation during this simulated summer day is 19.8 mm water equivalent. The contribution of sublimation to ablation is negligible; it is only −1 %.

In order to get an impression of the effect of the variability of the weather the experiment was repeated for a fine summer day (daily mean temperature 5° C, mean relative humidity 70 %, cloudiness 0.0 and wind velocity 2 m/s), and for a summer day with poor weather (−3° C, 95 %, 1.0 and 10.0 m/s for the same variables). The amounts of ablation appeared to be 29.4 and 2.3 mm water equivalent, respectively. The amount of ablation on the day with fine weather is 48 % larger than the amount of ablation on a day with 'climatological' weather (19.8 mm). Intuitively one might expect a larger difference. However, not all fine day factors contribute to a higher ablation. The low relative humidity and the low wind speed reduce the turbulent fluxes, while the incoming long wave radiation is reduced in the absence of clouds (see next subsection).

C. SENSITIVITY TO VARIATIONS OF THE METEOROLOGICAL INPUT PARAMETERS

Starting from the July 15 standard run discussed in subsection 5b, sensitivities to the variation of the input parameters were tested by varying one of the parameters in question, all other parameters being unchanged. This was done for (a) cloudiness, (b) relative humidity, (c) temperature and (d) wind velocity (see fig. 6a, b, c, d, respectively). In each case the upper panel shows the variations of the energy fluxes that are directly affected. The lower panels display the consequences for the amount of ablation.

An overcast sky reduces ablation by about a factor 2, due to a reduction of the incoming short wave radiation. This effect is counteracted to some extent by increasing long wave radiation.

Humidity mainly affects the latent heat flux. The higher the humidity, the larger the latent heat flux, of course. The sensitivity of net radiation to variations in humidity are negligible, because the sensitivities of short wave incoming and long wave incoming radiation almost cancel. Because of the effect of humidity on the latent heat flux the rate of formation of meltwater increases with relative humidity, inspite of the fact that sublimation is reduced or riming enhanced.

Fig. 6: Sensitivity of the directly affected daily averaged surface fluxes and ablation with cloudiness, humidity, temperature and wind velocity: Calculations are based on the Sonnblick climatology for July

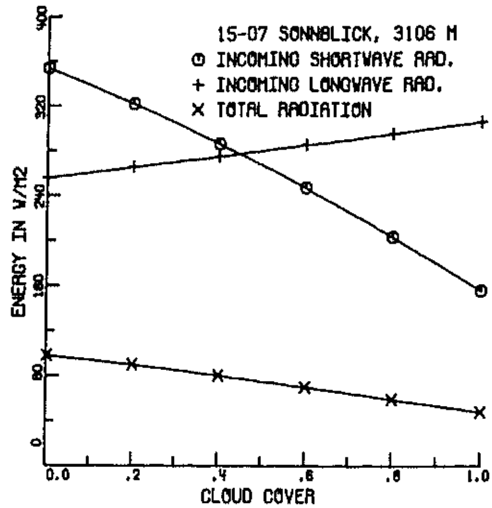

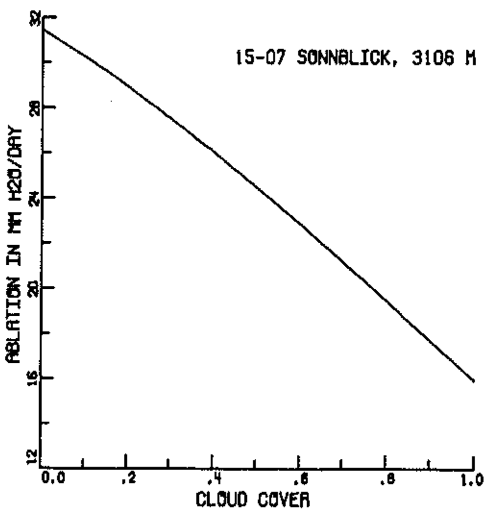

Fig. 6a

The effect of variations in daily mean temperature on ablation is quite complicated. This is mainly due to the reaction of the turbulent heat fluxes to changes in temperature. For temperatures below −7°C ablation is negligible. Between −7°C and 3°C the relation between temperature and ablation is nearly linear. If the temperature increases further, the stability of the atmosphere will start to suppress turbulence. With the prevailing wind velocity (5.1 m/s) turbulence completely disappeares when the

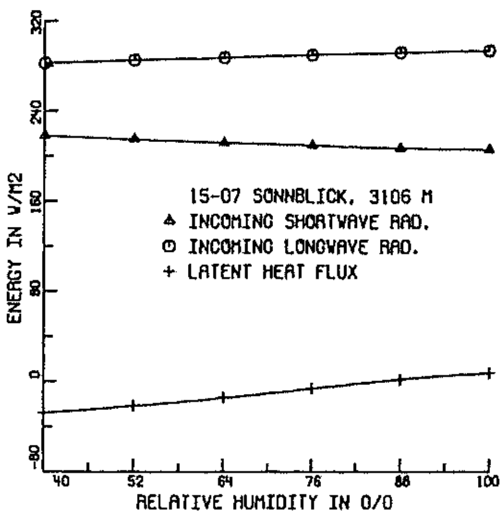

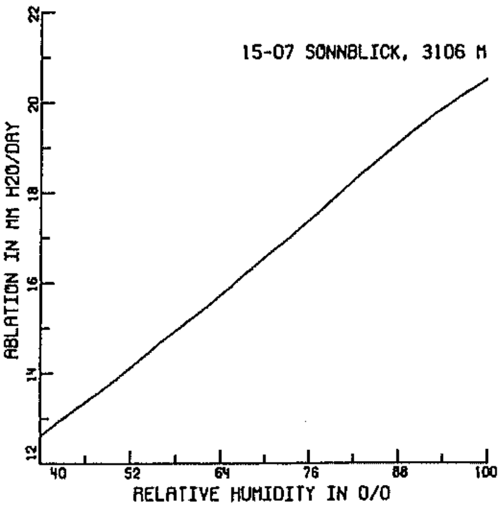

Fig. 6b

momentaneous temperature difference between screen height and surface exceeds about 6°C. If the daily mean temperature increases, the average turbulent flux mainly depends on the relative lengths of the periods with and without turbulence. For mean temperatures of about 8°C and higher the turbulent heat fluxes are zero throughout the day. The amount of ablation is then determined by the variation of the incoming long wave radiation.

The effect of variation in wind velocity is demonstrated in fig. 6d. For wind speeds below 3 m/s turbulence is absent during the entire day, so that variations in wind velocity do not affect ablation. For increasing wind velocities turbulent exchange

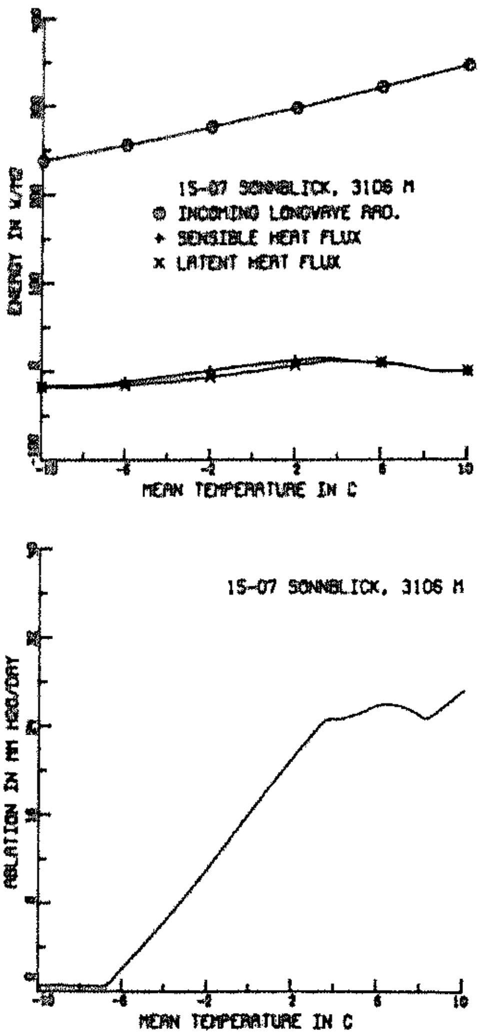

Fig. 6c

occurs during steadily increasing periods, untill turbulence is present during the entire day above about 5 m/s. Then ablation increases almost linearly with wind speed.

D. THE YEARLY CYCLE AT DIFFERENT ELEVATIONS

The second experiment presented here is a simulation of the yearly cycle of the mass balance for 5 different elevations (see fig. 7). The curves represent stable solutions. Solid curves were calculated with the M. O.-theory, dashed curves with the s. i.-theory. The noise in the curves during the accumulation season is due to the way the

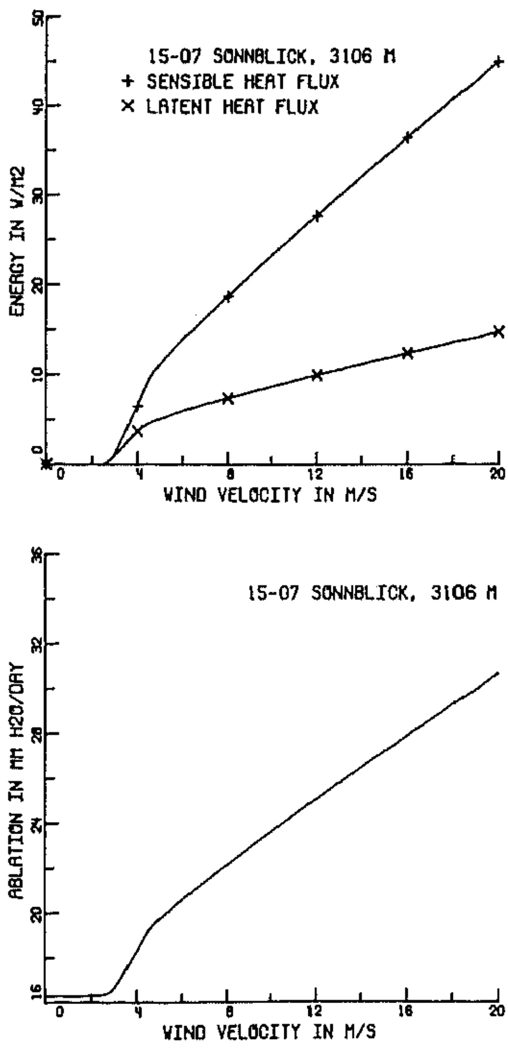

Fig. 6 d

precipitation is simulated. For both parameterizations no ablation at 3600 m is predicted. All precipitation (1495 mm water equivalent per year) is solid and all the meltwater formed at the surface during summer refreezes inside the glacier. At 3200 m (accumulation area) the winter cold wave is eliminated by refreezing meltwater at about July 1 and ablation takes place thereafter. The lower elevations are all in the ablation area. The lower the elevation, the larger the difference between the calculations with the M. O.-theory and the s. i.-theory. With the given wind velocity (5.1 ms^{-1}) the M. O.-theory predicts turbulence to vanish if the temperature at screen height exceeds the temperature at the glacier surface by more than about 6° C (see preceeding subsection). Of course, such very stable stratifications are more frequent at lower elevations. So, if the M. O.-theory is applied, the daily averaged transport of energy by turbulent fluxes during summer days may increase with elevation. However, the long wave incoming radiation decreases with elevation. This leads to nearly parallel curves for the elevations 2000 m, 2400 m and 2800 m. The main difference in net balance between these elevations is caused by different durations of the ablation season. If the s. i.-theory is applied the turbulent fluxes increase with decreasing elevation as they are simply proportional to the potential temperature difference. Apparently, the effect of the choice of the M. O.-theory or the s. i.-theory is considerable, certainly at lower elevations.

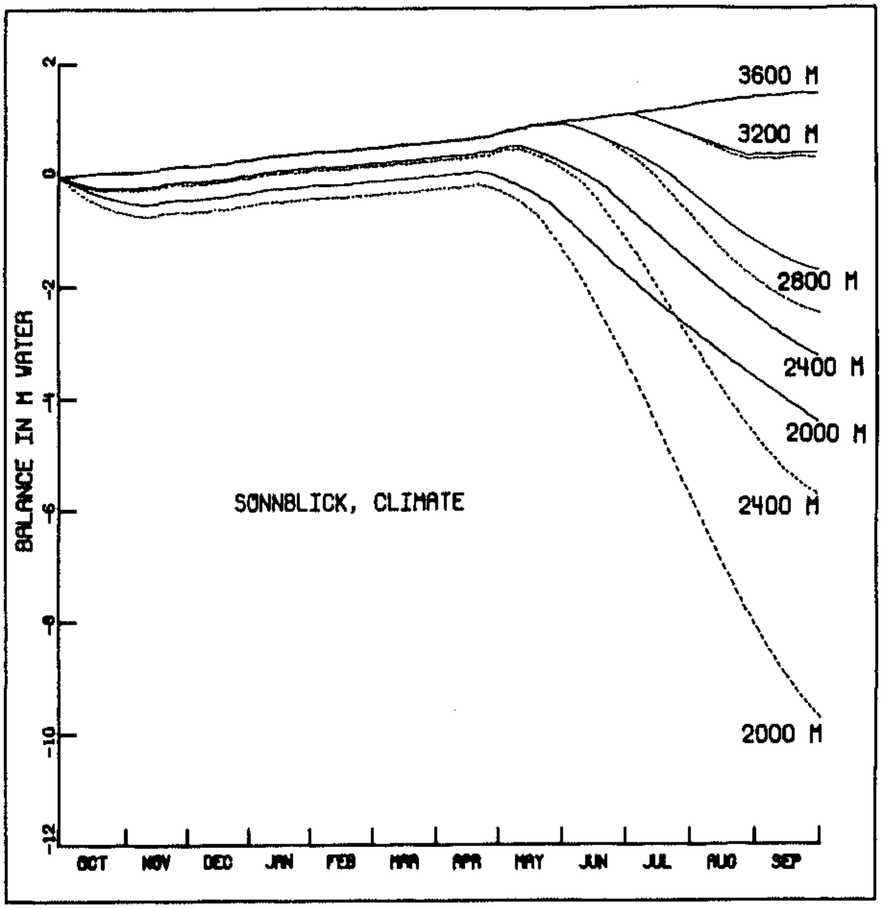

Fig. 7: Mass balance during a measurement year for five elevations ranging from 2000 till 3600 m, and for two different formulations of the turbulent fluxes (M. O.-theory = solid curves; s. i.-theory = dashed curves)

E. EFFECT OF A 'ZERO-DEGREE ASSUMPTION'

Most existing models presume that the snow/ice temperature remains at the melting point during all of the time under consideration. The advantage of these models is that calculations of temperature and density profiles of the glacier are not necessary. In order to assess the consequences of the 'zero-degree assumption', a one-year run of the present model with temperature and density profile calculations was compared to a run with the 'zero-degree assumption'. This was done for two elevations, one in the accumulation area (3200 m) and one in the ablation area (2500 m). Results are displayed in fig. 8. The columns represent mean ablation per day for every decade. In each column, the hatched area gives the ablation calculated with temperature and density profile computations included; the total area of each column represents the ablation obtained with the 'zero-degree assumption'. The amounts of ablation predicted under the 'zero-degree assumption' always exceed the amounts predicted by the present model.

There are two main reasons for the discrepancies. They are of different importance during different seasons. Under the 'zero degree assumption' ablation will immediately start when the total surface energy flux becomes-positive. In the complete model,

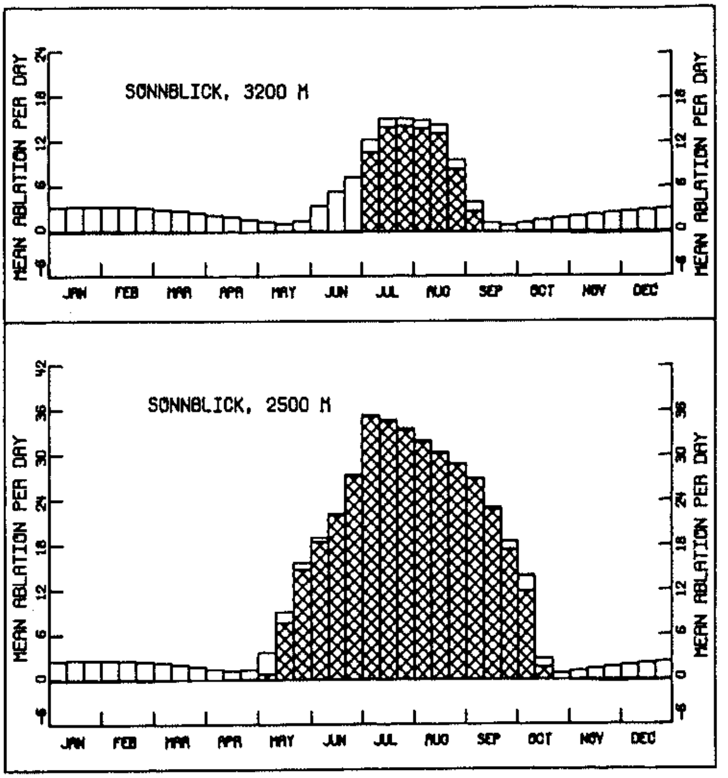

Fig. 8: Ablation per day in mm water equivalent averaged over decades. Total columns are calculations based on a 'zero degree assumption'; hatched areas refer to predictions made with temperature and density profile calculations

however, some of the energy will be used to heat the upper snow/ice layers by conduction and refreezing meltwater if the structure of the snow/ice permits penetration. This argument holds for both the warming of the upper layers before the start of the ablation season and in the morning during the ablation season. During winter both models predict no formation of meltwater. In that part of the year sublimation is the source of the different predictions. The lower the atmospheric temperature, the larger is the temperature gradient under the ‚zero-degree assumption'. Large amounts of evaporation are then predicted, whereas evaporation remains small when the temperature profile is calculated. At 3200 m the discrepancies between the two calculations are more serious. Because of lower atmospheric temperatures there, a stronger cold wave will penetrate the snow during the accumulation season, and also during the nights of the ablation season. More meltwater has to be spent to eliminate the cold wave. For the same reason, namely the lower temperatures, sublimation will be enhanced at 3200 m as compared to 2500 m. Some values of net calculated ablation are shown in table 2. As a matter of fact a model with a 'zero degree assumption' will not be used for calculation during the accumulation season. That is why the ablation figures for the ablation season only give a better comparison. In this context the ablation season is defined as the period during which melting is predicted under the 'zero degree assumption'. One can conclude that the 'zero degree assumption' is acceptable when the model is applied to an elevation of 2500 m. Predicted summer ablation is 103 % of the ablation obtained with temperature and density-profile calculations included. However, at 3200 m it fails (134 %). This is mainly due to overestimation of ablation in late May, June and early July.

Tab. 2: Comparison of net ablation with temperature and density profile calculations with net ablation under the 'zero degree assumption' in mm water equivalent. Values between parentheses are for the whole year; the other values are summer ablation only

	2500 m	3200 m
Profile calculations	3734 (3720)	798 (779)
Zero degree assumption	3862 (4226)	1071 (1639)

F. CONSEQUENCES OF A HEAVY SNOW FALL EVENT IN SUMMER

A major snow fall event during the ablation season will affect the net mass budget in two ways. In a direct way it is a contribution to summer accumulation; in an indirect way ablation is reduced by a higher albedo of the fresh snow. Fig. 9 demonstrates the impact on ablation of a fresh snow pack on July 30 at 2 elevations. Two cases are compared. In both cases, the weather on July 30 deviates from the climatological mean. Cloudiness was put equal to 1.0 and mean atmospheric temperature equal to $-2°C$ at both elevations. In the first case this day of bad weather remained dry (total columns); in the second case a heavy snow fall event (5 cm water equivalent) took place (hatched areas). Indeed, ablation was reduced in a significant way during the following days. In principle the impact is long lasting, because of the feedback mechanism higher albedo → less meltwater → lower densification rate (see equation 15) → higher albedo (see equation 7). At 2500 m, however, the reduction of the albedo is only present untill bare ice appears at the surface again at August 3. We found nearly the same amount of ablation reduction, namely some 8 cm water equivalent, at both altitudes.

Fig. 9: Ablation after a day with bad weather on July 30. Total columns are for the case of no solid precipitation, hatched areas represent the case that 5 cm water equivalent of snow fell on July 30

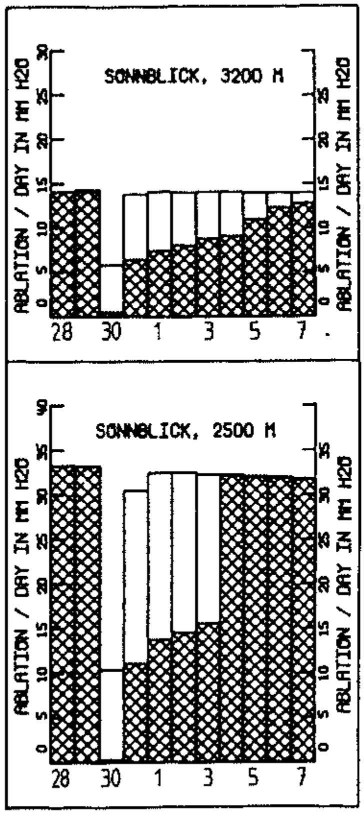

6. DISCUSSION

From fig. 6 the effect of variations in the meteorological input parameters (cloudiness, humidity, temperature and wind speed) on the energy fluxes and on ablation can be estimated. Whereas the relations between the energy fluxes and ablation (ordinate) and cloudiness and humidity (abscissa) approach linearity, the same cannot be said of the relation between the energy fluxes and ablation (ordinate) and temperature and wind velocity (abscissa). This deviation from linearity is considerable at the transition from a fully developed turbulent regime all through the day to a non-turbulent regime all through the day.

The sensitivity experiments presented in subsections 5d and 5e give some quantitative indication about the errors introduced by certain assumptions. From fig. 7 it becomes clear that the choice of the parameterization of the turbulent fluxes considerably affects the predicted net balance. The effect of this choice on the absolute value of net balance becomes larger for decreasing elevations. It is not within the scope of the present paper to present a discussion of the advantages and the limitations of the parameterizations of the turbulent fluxes presented here, but this point will presumably be taken up in future work. Fig. 7 is only meant to demonstrate the effect of the different parameterizations on the results.

If the aim of the model is to predict ablation, the 'zero degree assumption' seems to be valid for an elevation of 2500 m. As the winter and night cold wave will even be less at elevations lower than 2500 m the assumption can also be used there. However, at elevations higher than 2500 m the error in the calculation of mass balance will grow steadily with elevation. At 3200 m the ablation predicted under the 'zero degree assumption' is 134 % of the ablation computed with temperature and density calculations. At 3600 m the quotient of the predicted values is infinite, since all of the meltwater refreezes according to the present model (see fig. 7).

In subsection 5 f the impact of a heavy snow fall event (of 5 cm water equivalent) in summer was calculated. An estimate can be made of the amplification of the mass balance perturbation (2—3 times at both elevations). The amplification is due to the higher albedo of the fresh snow. Thus the calculations are strongly dependent on the way the albedo is parameterized. As this parameterization as well as the density (on which albedo is largely dependent) calculations are rather crude in the present model, one should be careful in interpreting the computed amplification. In a regression analysis of the mass balance of Hintereisferner (Austria), in which the mass balance is described as a linear function of summer temperature, summer precipitation (only solid) and winter precipitation, the amplification factor turned out to be 6.06 for all elevations (Letreguilly 1984).

Of course, the model presented here has other shortcomings as well. It is beyond the scope of this paper to treat them all in full detail. We will restrict ourselves to mention just a few of them:

- In the description of the evolution of the density profile no account has been taken of the horizontal and vertical inhomogeneities that are formed in the snow pack (see e. g. Higuchi and Tanaka 1982). These inhomogeneities are of great importance for the flow pattern of the meltwater, which in turn will affect the temperature distribution.
- In reality the energy fluxes between atmosphere and glacier are determined by the vertical profiles of variables like temperature and humidity. The parameterizations in this study, however, only use one temperature and one humidity to present the profiles. This will not so much affect the calculations of long runs, but may be a bad approximation for the simulation of a single day on which the vertical distribution of e. g. temperature strongly deviates from a standard profile of temperature.
- For the application of the M. O.-theory one has to assume a full adjustment of the atmospheric boundary layer considered (in this case the first 10 m above the surface) to the surface boundary conditions. This assumption is certainly not justified near the upwind edge of a glacier if the adjacent terrain is free from snow.

So far the model has not yet been tuned. Although we intend to do that in future, we expect that such a tuning will not affect the conclusions of the experiments presented here. The absolute value of the resulting mass balance figures will change, but the gradients and the differences of the results will hardly be affected.

ACKNOWLEDGEMENTS

This research is sponsored by the Ministery of Health and Environmental Protection (The Netherlands), under grant 611003.01.

REFERENCES

Ambach, W., 1965: Untersuchungen des Energiehaushaltes und des freien Wassergehaltes beim Abbau der winterlichen Schneedecke. Archiv für Meteorologie, Geophysik und Bioklimatologie B, 14 (2): 148—160.

Ambach, W., M. Blumthaler and P. Kirchlechner, 1981: Application of the gravity flow theory to the percolation of melt water through firn. Journal of Glaciology 27 (95): 67—75.

Braun, L. N., 1985: Simulation of Snowmelt-Runoff in Lowland and Lower Alpine Regions of Switzerland. Zürcher Geographische Schriften, Heft 21.

Businger, J. A., 1973: Turbulent transfer in the atmospheric surface layer. In: Workshop on micrometeorology, D. A. Haugen, Editor, Published by the American Meteorological Society.

Casinière, A. C. de la, 1974: Heat exchange over a melting surface. Journal of Glaciology 13 (67): 55—72.

Cehak, K. und J. Withalm, 1980: Über die Gültigkeit eines Markow-Ketten-Modells für Niederschlagsperioden im Hochgebirge. Meteorologische Rundschau 33: 148—155.

Dirmhirn, I. und E. Trojer, 1955: Albedountersuchungen auf dem Hintereisferner. Archiv für Meteorologie, Geophysik und Bioklimatologie B, 6: 375—379.

Dirmhirn, I. and F. D. Eaton, 1975: Some characteristics of the albedo of snow. Journal of Applied Meteorology 14: 375—379.

Escher-Vetter, H., 1980: Der Strahlungshaushalt des Vernagtferners als Basis der Energiehaushaltsberechnung zur Bestimmung der Schmelzwasserproduktion eines Alpengletschers. Münchener Universitätsschriften, Fachbereich Physik, Wissenschaftliche Mitteilung Nr. 39.

Geiger, R., 1966: The climate near the ground. Harvard University Press, Harvard, Massachusetts.

Harstveit, K., 1984: Snowmelt modelling and energy exchange between the atmosphere and a melting snow cover. Geophysical Institute, Meteorological Division, University of Bergen, Scientific Report No. 4.

Higuchi, K. and Y. Tanaka, 1982: Flow pattern of meltwater in mountain snow cover. IASH Publication no. 138: 63—69.

Hogg, I. G. G., J. G. Paren and R. J. Timmis, 1982: Summer heat and ice balances on Hodges Glacier, South Georgia, Falkland Islands Dependencies. Journal of Glaciology 28 (99): 221—238.

Hooke, R. L., J. E. Gould and J. Brzozowski, 1983: Near surface temperatures near and below the equilibrium line on polar and subpolar glaciers. Zeitschrift für Gletscherkunde und Glazialgeologie 19: 1—25.

Itier, B., 1980: Une méthode simplifiée pour la mesure du flux du chaleur sensible. Journal de Recherches Atmosphériques 14: 17—34.

Kimball, B. A., S. B. Idso and J. K. Aase, 1982: A model of thermal radiation from partly cloudy and overcast skies. Water Resources Research 18: 931—936.

Kojima, K., 1967: Densification of seasonal snow cover. In: Physics of snow and ice, Proceedings of the International Conference on Low Temperature Science, part 2: 929—952.

Kraus, H., 1972: Energy exchange at air-ice interface. IASH Publication No. 107: 128—164.

Letreguilly, A., 1984: Bilans de masse des glaciers alpins: methods de mesure et repartition spatio-temporelle. Publication no. 439 du Laboratoire de Glaciologie, Grenoble.

Meyers, T. P. and R. F. Dale, 1983: Predicting daily insolation with hourly cloud height and coverage. Journal of Climate and Applied Meteorology 22 (4): 537—545.

Paterson, W. S. B., 1981: The physics of glaciers, 24d ed., Oxford, Pergamon Press, 380 pp.

Sauberer, F., 1955: Zur Abschätzung der Globalstrahlung in verschiedenen Höhenstufen der Ostalpen. Wetter und Leben 7: 22—29.

Smith, W. L., 1966: Note on the relationship between total precipitable water and surface dewpoint. Journal of Applied Meteorology 5: 726—727.

Wagner, H. P., 1980: Strahlungshaushaltsuntersuchungen an einem Ostalpengletscher während der Hauptablationsperiode. Teil II. Langwellige Strahlung und Strahlungsbilanz. Archiv für Meteorologie, Geophysik und Bioklimatologie 28: 41–62.
Wallen, C. C., 1977: Climates of Central and Southern Europe. World Series of Climatology, Vol. 6, Elsevier Scientific Publishing Company.

Manuscript received October 16, 1985

Authors' address: W. Greuell and J. Oerlemans
Institute of Meteorology and Oceanography
University of Utrecht
Princetonplein 5
3584 CC Utrecht
The Netherlands